

RESEARCH ARTICLE

Physical Layer Evaluation on IEEE 802.11p With Different Configurations in NLOS Scenarios for V2V Communications

SHUTING GUO^{1,2}, DANIEL N. ALOI¹, (Senior Member, IEEE),
JIA LI¹, (Senior Member, IEEE), AND HONGMEI ZHAO^{1,2}

¹Department of Electrical and Computer Engineering, Oakland University, Rochester, MI 48309, USA

²College of Electrical and Information Engineering, Zhengzhou University of Light Industry, Zhengzhou, Henan 450002, China

Corresponding author: Daniel N. Aloï (aloi@oakland.edu)

ABSTRACT Motivated by the evolution of vehicular technologies and applications, the vehicle-to-everything (V2X) communications can be realized by the dedicated short-range communications (DSRC) and cellular V2X (C-V2X) which are undergoing continuous and widespread development. As the first standardized DSRC technology, IEEE 802.11p, that has been studied with large-scale field trials performed worldwide, is more mature and robust than the other V2X technologies. The main contributions of the proposed work over previous work are listed as follows. Firstly, to break the limitation of partial physical layer (PHY) evaluation, extensive PHY metrics, which include the packet error rate (PER), packet reception ratio (PRR), output packet inter-arrival time (IAT), and output effective data rate, are adequately employed to fulfill complete PHY evaluation. Secondly, to avoid incomplete analysis on antenna configurations, various multi-antenna configurations, containing the multiple-input multiple-output (MIMO), single-input multiple-output (SIMO), and multiple-input single-output (MISO) systems, are involved together with the single-input single-output (SISO) configuration to realize comprehensive analysis on diverse antenna configurations. Finally, to overcome unobvious exhibition on effect of parameters on PHY performance, considerably different packet sizes and modulation and coding schemes (MCSs) are investigated under the urban non-line-of-sight (NLOS) and highway NLOS scenarios to disclose the deep impact of each parameter. Important conclusions from a thorough MATLAB-based PHY simulation are summarized as follows. Firstly, in comparison with the SISO system, the multi-antenna systems are more favorable in reducing the PER, increasing the PRR and transmission coverage, decreasing the output packet IAT, and elevating the output effective data rate, below the signal-to-noise ratio (SNR) threshold and above the distance threshold. Secondly, the packet size and the MCS should be determined suitably to adapt to the high-reliability, low-latency, or high-throughput requirement in different applications. Finally, compared to the highway NLOS scenario with higher Doppler effect, the urban NLOS scenario is more tolerant to the larger packet and higher MCS in the vehicle-to-vehicle (V2V) communications with its lower PER, larger PRR and transmission coverage, smaller output packet IAT, and higher output effective data rate.

INDEX TERMS IEEE 802.11p, MIMO, physical layer evaluation, V2V.

I. INTRODUCTION

Focused on the vehicle-to-everything (V2X) communications which can improve road safety, energy efficiency, traffic management, and pollution reduction, the U.S. Federal

The associate editor coordinating the review of this manuscript and approving it for publication was Luyu Zhao¹.

Communications Commission (FCC) allocated a specific 75 MHz licensed spectrum in the 5.9 GHz frequency band from 5.850 GHz to 5.925 GHz in 1999 for the intelligent transportation system (ITS) to support both the vehicle-to-vehicle (V2V) and vehicle-to-infrastructure (V2I) communications by reducing possible interference with other wireless devices [1], [2]. Over the past two decades, this

allocation has sparked major research activities around the world to develop and deploy V2X communications aimed at providing multiple challenging services, such as safety to vulnerable road users (VRU), smart navigation, cooperative maneuvering, and connected autonomous driving [3].

The radio access technologies (RATs), which can be divided into dedicated short-range communications (DSRC) and cellular V2X (C-V2X), are undergoing continuous and widespread evolution for more stringent vehicular scenarios and applications where the high-reliability, low-latency, or high-throughput requirement needs to be satisfied [4], [5]. The DSRC operates within the 5.9 GHz frequency band primarily, however, the C-V2X can operate not only in the 5.9 GHz frequency band but also in the licensed operating bands of the cellular operators [4].

IEEE 802.11p was the first standardized DSRC technology for direct V2X communications [6] and followed by the long-term evolution (LTE) announced by the 3rd Generation Partnership Project (3GPP) in Release 14 with advanced features based on cellular technologies [7]. On one hand, IEEE 802.11bd was released as the next-generation V2X (NGV) standard for the DSRC [8], [9] and introduces new physical layer (PHY) and medium access control (MAC) technologies which should bring better performance compared with IEEE 802.11p. On the other hand, the new radio V2X (NR-V2X) was issued as the next-generation C-V2X and fully specified in Release 16 which supports various use cases, multiple deployment options, and wide frequency bands with flexible, scalable, and forward-compatible PHY and MAC layers [10], [11].

With short-range wireless technologies in the DSRC, direct communication can be realized between vehicles, infrastructures, and pedestrians, and their awareness range can be extended greatly beyond autonomous on-board capabilities [12]. As a primary competitor to IEEE 802.11p in the C-V2X, the LTE-V2X suffers from the challenge in transmitting data within permissible latency with higher cellular network traffic load [13], [14], [15]. Moreover, even if IEEE 802.11p had evolved to IEEE 802.11bd for the sake of enhancements on IEEE-based V2X communications [16], [17], the next-generation technology cannot be seamlessly embraced in future application scenarios until its standardization and test have been finished [1]. Furthermore, compared to the other V2X technologies for which complete verification is further needed on their effective reliability and scalability [14], IEEE 802.11p is more mature and robust with large-scale field trials performed worldwide [14], [16], [18]. Hence, our previous work on IEEE 802.11bd in [19] is followed by this proposed work on IEEE 802.11p which complements fundamental analysis on the DSRC.

II. LITERATURE REVIEW

Several existing literatures are listed below which are dedicated to the DSRC and the C-V2X protocols for their performance estimation.

The simulation and measurement with two antenna types located at three different heights were implemented in [20] with the C-V2X PC5 mode 4 interfaces under a rural scenario for direct V2V communications. Additionally, the PHY performance comparison on both C-V2X standards and both DSRC standards was conducted in [21] according to the simulation on the V2V channel model under an urban non-line-of-sight (NLOS) scenario. Furthermore, it was indicated in [22] that, instead of a higher packet delivery ratio (PDR) and a smaller end-to-end delay which can be realized with the DSRC technology in the observed V2I scenarios, the worse performance with the LTE technology appends additional limitations to the feasible applications. Moreover, under the highway scenarios in [23] where the system-level simulation is fulfilled, the DSRC is superior to the LTE for higher vehicle density due to the smaller and stable data packet delay. In addition, the performance analysis on IEEE 802.11p and IEEE 802.11bd was proposed in [17] across multiple layers including the PHY for safety applications. Besides, the real-world performance of IEEE 802.11p was analyzed in [2] focusing on the maximum range and the PDR of V2I communications. Moreover, complete PHY evaluation on IEEE 802.11bd was presented in [19] with various antenna configurations, packet sizes, and modulation and coding schemes (MCSs) under both the urban NLOS and highway NLOS scenarios.

Nevertheless, some gaps are present in previous work for IEEE 802.11p and should be bridged to improve its performance estimation. Faced with the packet error rate (PER) and packet reception ratio (PRR) under a single-input single-output (SISO) channel of the highway line-of-sight (LOS) and NLOS scenarios with fixed packet size and MCS in [24], not only the PHY performance regarding the latency and throughput, but also the impact of the multi-antenna configuration which contains the multiple-input multiple-output (MIMO), single-input multiple-output (SIMO), and multiple-input single-output (MISO), Doppler effect, packet size, and MCS cannot be realized in the investigation. Since the PER and throughput considered in [16] are under the SISO channel model either for MCS 2 with the 100-byte packet or for MCS 5 with the 300-byte packet, the PRR and latency metrics are absent and the effect of the multi-antenna configuration, MCS, and packet size are not discussed. Although the PER, PRR, data rate, and packet inter-arrival time (IAT) are adequately selected as the PHY metrics in [21] for an urban NLOS scenario with the SISO channel model, the highway NLOS scenario and the MIMO, SIMO, and MISO channel models are still indispensable to explore the influence of the Doppler effect and multi-antenna configuration on the PHY performance.

The main contributions of this proposed work are summarized as follows. Firstly, to break the restriction of partial PHY evaluation induced by limited metrics chosen in most previous literatures, extensive PHY metrics, which include the PER, PRR, output packet IAT, and output effective data rate, are sufficiently adopted to guarantee thorough PHY

TABLE 1. Comparison between this work and existing work.

Source	PHY Metric				Parameter			
	PER	PRR	Output Packet IAT	(Output) Effective Data Rate	Antenna Configuration	Packet Size (bytes)	MCS	V2V Scenario
[24]	Yes	Yes	No	No	SISO	300	2	Highway LOS Highway NLOS
[16]	Yes	No	No	Yes	SISO	100	2	Rural LOS Urban LOS
						300	5	Highway LOS Urban NLOS Highway NLOS
[21]	Yes	Yes	Yes	Yes	SISO	100 1500	2/0 6	Urban NLOS
This Work	Yes	Yes	Yes	Yes	SISO MISO SIMO MIMO	100 1500	2 6	Urban NLOS Highway NLOS

evaluation on IEEE 802.11p. Secondly, to remedy incomplete analysis on antenna configurations caused by single SISO configuration selected in numerous existing studies, various multi-antenna configurations, containing the MIMO, SIMO, and MISO systems, are added to fully investigate the difference between the multi-antenna and single-antenna configurations. Finally, to overcome unobvious effect brought by fixed parameter or slightly different parameters utilized in some prior research, considerably different packet sizes and MCSs are studied by means of the ultra-reliable low-latency communications (URLLC) and enhanced mobile broadband (eMBB) applications with rather low and high MCSs for the urban NLOS and highway NLOS channel models under the V2V scenarios to deeply uncover the impact of each parameter on the PHY performance.

The detailed comparison between this work and the previous work is outlined in Table 1 which can explicitly clarify the advantages of the proposed work over the existing work.

The subsequent organization of the paper is arranged as follows. The IEEE 802.11p, orthogonal frequency-division multiplexing (OFDM) and MIMO, PHY metrics, and LOS and NLOS propagations, are overviewed in Section III for fundamental introduction on the theories and methods. The complete PHY evaluation on IEEE 802.11p is performed and analyzed in Section IV with a MATLAB-based simulation according to multiple PHY metrics by means of diverse configurations and different scenarios. Finally, the conclusion of the paper is provided in Section V which discloses the significant findings of the proposed work.

III. THEORIES AND METHODS

A. IEEE 802.11P

As an improved IEEE 802.11 protocol completed in 2010, IEEE 802.11p standard is used to describe the PHY and MAC layers for interchanging wireless broadcast messages in vehicular communications with an allocation of the 75 MHz

bandwidth at the designated 5.850 – 5.925 GHz frequency band [13].

By halving the channel bandwidth from 20 MHz to 10 MHz and increasing the carrier frequency from 5 GHz to 5.9 GHz, with all the corresponding doubled timing OFDM parameters, the IEEE 802.11p was derived from the Wi-Fi standard, IEEE 802.11a, which was designed for short-range, low-mobility, and indoor applications, to meet the requirements on longer range, extreme-high mobility, and rapid-changing channel conditions [2], [25].

The crucial PHY parameters of IEEE 802.11p and IEEE 802.11a are compared in Table 2 [6] where the guard interval (GI) within the OFDM symbol duration is given simultaneously.

In the light of the channel conditions, distance from transmitter to receiver, and quality of service (QoS) requirements such as reliability, transmission coverage, latency, and throughput [19], an appropriate MCS should be selected for efficient transmission from eight possible MCSs ranging from 0 to 7 which represent different combinations of modulation and coding rate, as outlined in Table 3 [6].

B. OFDM AND MIMO

1) OFDM MODULATION SCHEME

In wireless communications where reflection, diffraction, and scattering are the dominant radio-propagation mechanisms, delay spread is caused by multipath propagation and the inter-symbol interference (ISI) is generated by time dispersion in the wireless channel [26], [27]. According to the OFDM modulation scheme employed on the IEEE 802.11p PHY, the entire wide-band channel over which the high-rate data stream is transmitted is partitioned into multiple narrow-band subchannels whose bandwidth is smaller than the channel coherence bandwidth [28], [29]. Hence, the frequency-selective-fading channel is transformed into many flat-fading subchannels which are more robust against the multipath fading [29], [30], [31]. Based on the parallel

TABLE 2. PHY comparison between IEEE 802.11a and IEEE 802.11p.

Parameter	IEEE 802.11a	IEEE 802.11p
Data Subcarriers	48	48
Pilot Subcarriers	4	4
Null Subcarriers	12	12
Total Subcarriers	64	64
Channel Bandwidth	20 MHz	10 MHz
Subcarrier Spacing	20 MHz/64=312.5 KHz	10 MHz/64=156.25 KHz
OFDM Symbol Duration	4 μ s (800 ns GI)	8 μ s (1.6 μ s GI)

TABLE 3. MCS options, data rates, and transmission latencies of IEEE 802.11p.

MCS	Modulation	Coding Rate	Theoretical Data Rate (Mbps)	Actual Data Rate (Mbps)		Transmission Latency (ms)	
				100 bytes	1500 bytes	100 bytes	1500 bytes
0	BPSK	1/2	3.00	2.33	2.95	0.344	4.07
1	BPSK	3/4	4.50	3.13	4.37	0.256	2.74
2	QPSK	1/2	6.00	3.85	5.79	0.208	2.07
3	QPSK	3/4	9.00	4.76	8.52	0.168	1.41
4	16-QAM	1/2	12.00	5.56	11.19	0.144	1.07
5	16-QAM	3/4	18.00	6.67	16.13	0.120	0.744
6	64-QAM	2/3	24.00	7.14	20.83	0.112	0.576
7	64-QAM	3/4	27.00	7.69	23.08	0.104	0.520

transmission over the overlapping orthogonal subcarriers which can provide high spectral efficiency [3], the high-data-rate transmission can be guaranteed, meanwhile, the symbol duration can be increased to alleviate the time dispersion and resulting ISI in the multipath channel [31], [32], [33], [34].

A cyclic prefix (CP) is appended to an OFDM symbol by replicating a segment from the end of the OFDM symbol to the beginning of the symbol [35], and the CP duration should be longer than the maximum delay spread to mitigate the ISI in the multipath channel [29], [31], [34], [36]. With the cyclic extension of the OFDM symbol, the linear convolution between transmitted signal and channel impulse response in single-carrier system is converted into the circular convolution in multi-carrier system, which is significant to maintain the subcarrier orthogonality [29], [30], [37]. Accordingly, compared to the single-carrier system which requires complex time-domain equalizer, the simpler per-subcarrier equalizer is performed in frequency domain for the multi-carrier system to offset the distortion induced by the channel [31], [34], [37], [38].

Since there are 64 subcarriers included in a single OFDM symbol of IEEE 802.11p, a 64-point inverse fast Fourier transform (IFFT) performed at the OFDM modulator in the transmitter and a 64-point fast Fourier transform (FFT) at the OFDM demodulator in the receiver are combined so that the efficient implementation integrated into commercial hardware can be guaranteed [34], [37], [39].

The architecture of the OFDM modulation scheme is described in Fig. 1 [29], [34], [37], [40] where S/P and P/S represent the serial-to-parallel convertor and parallel-to-serial convertor respectively.

2) MULTI-ANTENNA CONFIGURATIONS

According to the deployment of multiple antennas on one side or both sides of the communication link, the multi-antenna configurations, which contain the MIMO, SIMO, and MISO, can improve the bit error rate (BER) and/or data rate without consuming any additional transmit power and bandwidth compared to the SISO configuration [29], [32], [41]. Instead of combating the multipath property of the wireless channel, the MIMO, SIMO, and MISO systems exploit the multipath to increase the signal-to-noise ratio (SNR) and thus the channel capacity, and to improve the reliability, coverage, and throughput by sharing the communication resources not only in the time and frequency domain, but also in the space domain [28], [34].

Three multi-antenna techniques, which include spatial diversity, spatial multiplexing, and beamforming, are respectively utilized to obtain diversity gain, multiplexing gain, and array gain [28], [29], [41], in which there is a trade-off strategy between the diversity gain and the multiplexing gain to accommodate specific requirement for different applications [29], [42].

A continuous-time MIMO system model which is composed of N_T transmit antennas and N_R receive antennas is demonstrated in Fig. 2 [19], [28], [42].

The received signal of the continuous-time MIMO system can be expressed as [40]

$$\mathbf{y}(t) = \int_{-\infty}^{\infty} \mathbf{H}(\tau)\mathbf{x}(t - \tau)d\tau + \mathbf{v}(t), \quad (1)$$

where $\mathbf{y}(t)$ is the $N_R \times 1$ received signal vector, $\mathbf{H}(t)$ is the $N_R \times N_T$ normalized channel matrix, $\mathbf{x}(t)$ is the

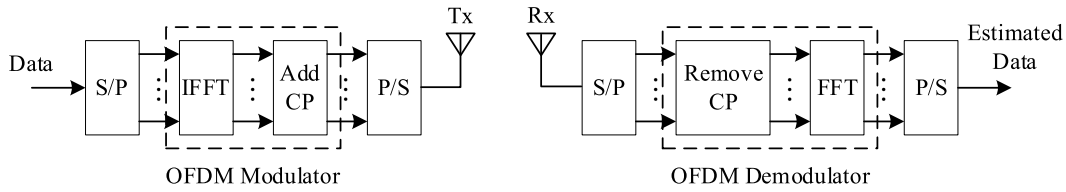


FIGURE 1. OFDM modulation scheme.

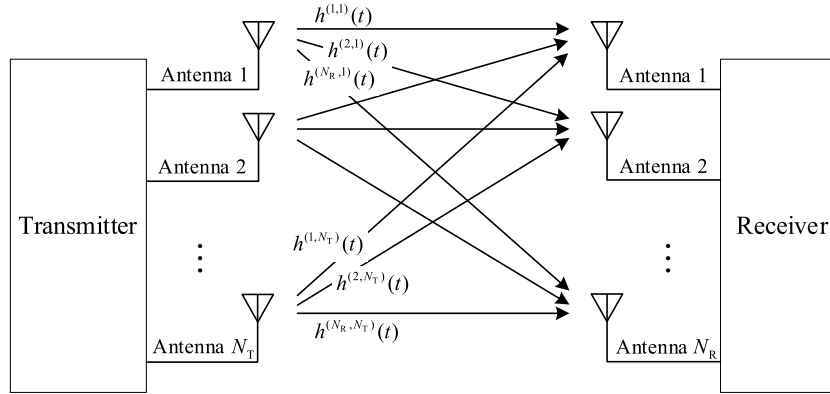


FIGURE 2. MIMO system model.

$N_T \times 1$ transmitted signal vector, and $\mathbf{v}(t)$ is the $N_R \times 1$ noise vector, respectively.

Accordingly, the received signal of the discrete-time MIMO system can be expressed as [40]

$$\mathbf{y}[n] = \sum_{l=0}^L \mathbf{H}[l]\mathbf{x}[n-l] + \mathbf{v}[n], \quad (2)$$

where $\mathbf{y}[n]$, $\mathbf{H}[n]$, $\mathbf{x}[n]$, and $\mathbf{v}[n]$ are the received signal vector, normalized channel matrix, transmitted signal vector, and noise vector, which have been discretized respectively.

If the channel tap number L is equal to 0, the input-output relationship on the flat-fading MIMO channel can be derived from the reduction of the frequency-selective-fading MIMO channel and expressed as [40]

$$\mathbf{y}[n] = \mathbf{H}\mathbf{x}[n] + \mathbf{v}[n]. \quad (3)$$

3) MIMO-OFDM SCHEME

Since most of the MIMO techniques are explored for the flat-fading channel, the OFDM scheme which provides narrowband flat-fading channel can be integrated into the MIMO technique to support the transmission over wideband frequency-selective-fading channel [29], [33], [38], [41]. Each subcarrier can be modeled as an independent MIMO system in the OFDM-based transmission, consequently, the MIMO-OFDM receiver can be simplified due to the operation on the independent subcarriers when the CP is long enough to eliminate the time dispersion of the multipath channel [34].

Different from the transmitted signals generated from the OFDM transmitter which can only be constructed within

a symbol-subcarrier grid on the time-frequency plane, the output signals of the MIMO encoder can be represented in either space-time plane, or space-frequency plane, or space-time-frequency plane in the MIMO-OFDM system by virtue of the introduction of a third spatial dimension which provides more implementation flexibility [30]. Based on the combination of the OFDM scheme and the MIMO technique, high-speed wireless communications can be maintained by taking advantage of the benefits of both technologies with further improved performance [30], [41].

The architecture of the MIMO-OFDM scheme with N_T transmit antennas and N_R receive antennas is portrayed in Fig. 3 [30], [34], [40], [41].

C. PHY METRICS

1) PER

To describe the communication reliability which represents the receiver performance, the PER is defined as the most usual PHY metric which is the percentage of erroneously received packets to total transmitted packets [3], [19], [21]. As a function of transmitted SNR with a logarithmic scale, lower PER corresponds to higher reliability of communication.

2) PRR

Contrary to the definition of the PER, the PRR refers to the percentage of successfully received packets to total transmitted packets which indicates the likelihood of successful transmissions [3], [19], [21]. As a function of distance between transmitter and receiver on a non-logarithmic scale, higher PRR implies higher possibility

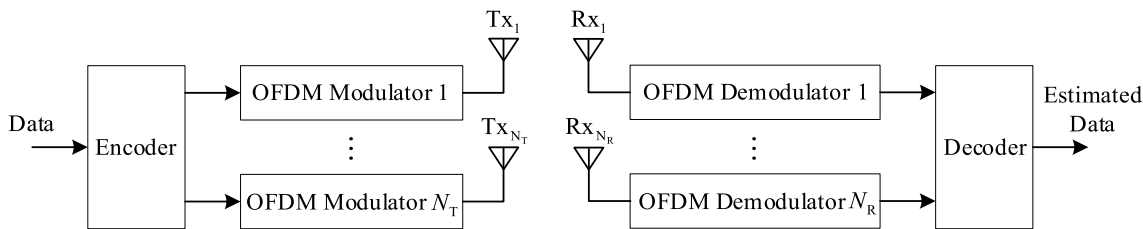


FIGURE 3. MIMO-OFDM scheme.

of successful communication and thus higher reliability of the link. Transmission coverage, which is utilized to measure the maximum communication range, is defined as the transmission distance at which the desired link-level PRR, such as 90%, can be met to satisfy the rigorous requirement on reliability in most vehicular applications [19].

In the high-reliability applications where the PER can be greatly reduced and the PRR can be extremely increased, the effective communication range can be highly extended and thus the transmission coverage with the specific PRR requirement can be significantly increased accordingly. Consequently, the large-coverage requirement can be satisfied simultaneously in ultra-reliable communications.

3) TRANSMISSION LATENCY AND PACKET IAT

a: TRANSMISSION LATENCY

The transmission latency is also termed as packet duration and defined as the required time of the PHY to transmit an IEEE 802.11p packet on wireless medium which can generate a significant influence on the end-to-end latency [21]. It can be expressed as [3], [21], [43]

$$T_{tx}^{11p} = T_{pre}^{11p} + T_{AIFS}^{11p} + T_{sym}^{11p} \cdot N_{sym}^{11p}, \quad (4)$$

where $T_{pre}^{11p} = 40 \mu s$ is the duration of the Preamble field and the SIGNAL field [6], $T_{AIFS}^{11p} = 32 \mu s$ is the arbitrary inter-frame space (AIFS) for priority data [19], $T_{sym}^{11p} = 8 \mu s$ is the duration of an OFDM symbol, and N_{sym}^{11p} is the required number of the OFDM symbols obtained by [3]

$$N_{sym}^{11p} = \left\lceil \frac{P_b \cdot 8}{N_{sd}^{11p} \cdot R^{11p} \cdot N_{bpsc}^{11p}} \right\rceil, \quad (5)$$

where P_b is the payload size in bytes which measures the data carried in a packet, $N_{sd}^{11p} = 48$ is the number of data subcarriers in an OFDM symbol, R^{11p} is the coding rate, N_{bpsc}^{11p} is the coded bits per subcarrier, and $\lceil \cdot \rceil$ is a ceiling function applied to round up values to the nearest integer.

The transmission latencies are compared in Table 3 with the 100-byte packet and 1500-byte packet for all MCSs.

b: PACKET IAT

To measure the time interval between two successive successful packet receptions, the packet IAT is calculated

by dividing the packet transmission latency with the PRR, at each given distance for each MCS in actual communication where the nonzero PER must be considered [19], [21].

4) THEORETICAL DATA RATE, ACTUAL DATA RATE, AND EFFECTIVE DATA RATE

As the crucial metric to estimate the speed of data transmission in wireless communications, data rate is known as the number of transmitted data bits per second and measured in bits per second (bps).

a: THEORETICAL DATA RATE

The theoretical data rate of IEEE 802.11p is calculated as the division between the data bits carried by an OFDM symbol and the OFDM symbol duration [3], [6]. Since the overhead is not taken into consideration, the theoretical data rate is an ideal maximum data rate but can never be reached in real communication.

The theoretical data rates ranging from 3 Mbps to 27 Mbps are listed in Table 3 for all MCSs [6].

b: ACTUAL DATA RATE

The overhead, which includes a preamble within each packet and at least an inter-frame space (IFS) between successively transmitted packets, is present in the transmitted PHY frame, which is indispensable for the data transmission [3], [19]. Therefore, the actual data rate is calculated by dividing the data bits transmitted by a packet with the packet duration and is the maximum effective data rate which can be realized in real communication when all the transmitted packets are successfully received. Accordingly, the actual data rate can be obtained by means of the payload size P_b and transmission latency T_{tx}^{11p} with [3], [21]

$$\Gamma^{11p} = \frac{P_b \cdot 8}{T_{tx}^{11p}}. \quad (6)$$

The fixed overhead occupied in the packet results in the difference between the actual data rate and the theoretical data rate, and their gap which is dominated by the variable payload size is reduced in larger packet and increased in smaller packet [3], [19], [21].

The actual data rates are supplied in Table 3 with the 100-byte packet and 1500-byte packet for all MCSs.

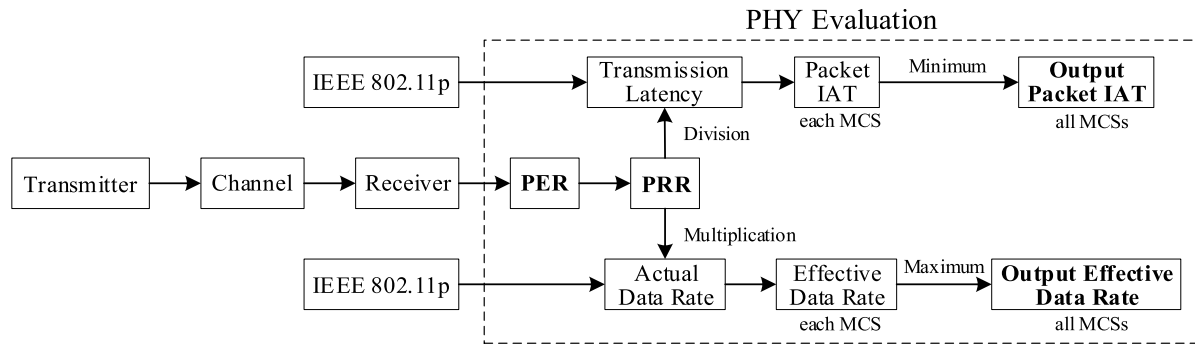


FIGURE 4. Simulation framework.

c: EFFECTIVE DATA RATE

In a practical communication link where the PER is nonzero generally, the effective data rate is obtained by the multiplication of the actual data rate and the PRR for each MCS, at each given distance [19].

D. LOS AND NLOS PROPAGATIONS

In contrast to the LOS propagation where there exists direct path travelling from transmitter to receiver which experiences the shortest possible distance [26], the NLOS propagation occurs when there are obstacles existing which block direct communication but preserve indirect communication between the transmitter and receiver. Along multiple paths generated in the reflection, diffraction, and scattering mechanisms induced by an encounter with the obstacles, the fluctuation on power of the received signal takes place in space, and/or in frequency, and/or in time, due to angle spread, delay spread, and Doppler spread respectively, according to the random superposition of all multipath components [19]. As a result, in addition to scarce available bandwidth, path loss, co-channel interference, and noise which are typical impairments in the LOS propagation of the wireless channel, the other impairments, for example, the multipath fading that is composed of severe fluctuations in the received signal, also exist during the NLOS propagation [19].

Based on the multipath taps over which the direct signal and the reflected/diffracted/scattered signals are characterized by power, root mean square (RMS) delay spread, and Doppler spread obtained by merging the results of different real-world measurement campaigns for usual V2V scenarios, the general V2V radio channel models are established for the rural LOS, urban approaching LOS, urban crossing NLOS, highway LOS, and highway NLOS scenarios respectively [44] and widely employed in the PHY simulation.

With more rich multipath components, the NLOS propagation suffers from more serious multipath fading which is challenging for the desired high-performance communications. However, the multi-antenna systems can leverage the multipath effect to improve the performance of wireless communications and thus generate more significant promotion

TABLE 4. Simulation parameters.

Parameter	IEEE 802.11p
Transmit Power	23 dBm
Tx Antenna Gain	3 dB
Rx Antenna Gain	3 dB
Reference Path Loss	47.86 dB (at 1 m)
Path-loss Exponent	2.75
Noise Power	-104 dBm
Noise Figure	9 dB
Packet Size	100 bytes (URLLC), 1500 bytes (eMBB)
V2V Channel Model	Urban NLOS, Highway NLOS
Channel Bandwidth	10 MHz
Carrier Frequency	5.9 GHz

in the NLOS propagation than in the LOS propagation [45]. Accordingly, the urban NLOS and highway NLOS channel models provided in [44] instead of the LOS channel models are analyzed in the simulation to explicitly demonstrate the superiority of the multi-antenna configurations.

IV. RESULTS

According to the MATLAB-based simulation on complete PHY modeling [46], [47], the PHY performance of IEEE 802.11p is evaluated based on different parameters by means of various metrics for the V2V communications.

The framework of implementation on the simulation with parameters summarized in Table 4 is displayed in Fig. 4.

A. PER

With the given antenna, packet, and MCS configurations in both NLOS scenarios, the simulation results of the PER are displayed in Fig.5 where there are merely MCS 2 and MCS 6 presented for clarity and simplicity.

1) IMPACT OF ANTENNA CONFIGURATION

a: SISO

Due to a single transmit antenna and a single receive antenna which result in an absence of any diversity, the worst performance is revealed in the SISO (1 × 1) system with the highest PER from all the antenna configurations.

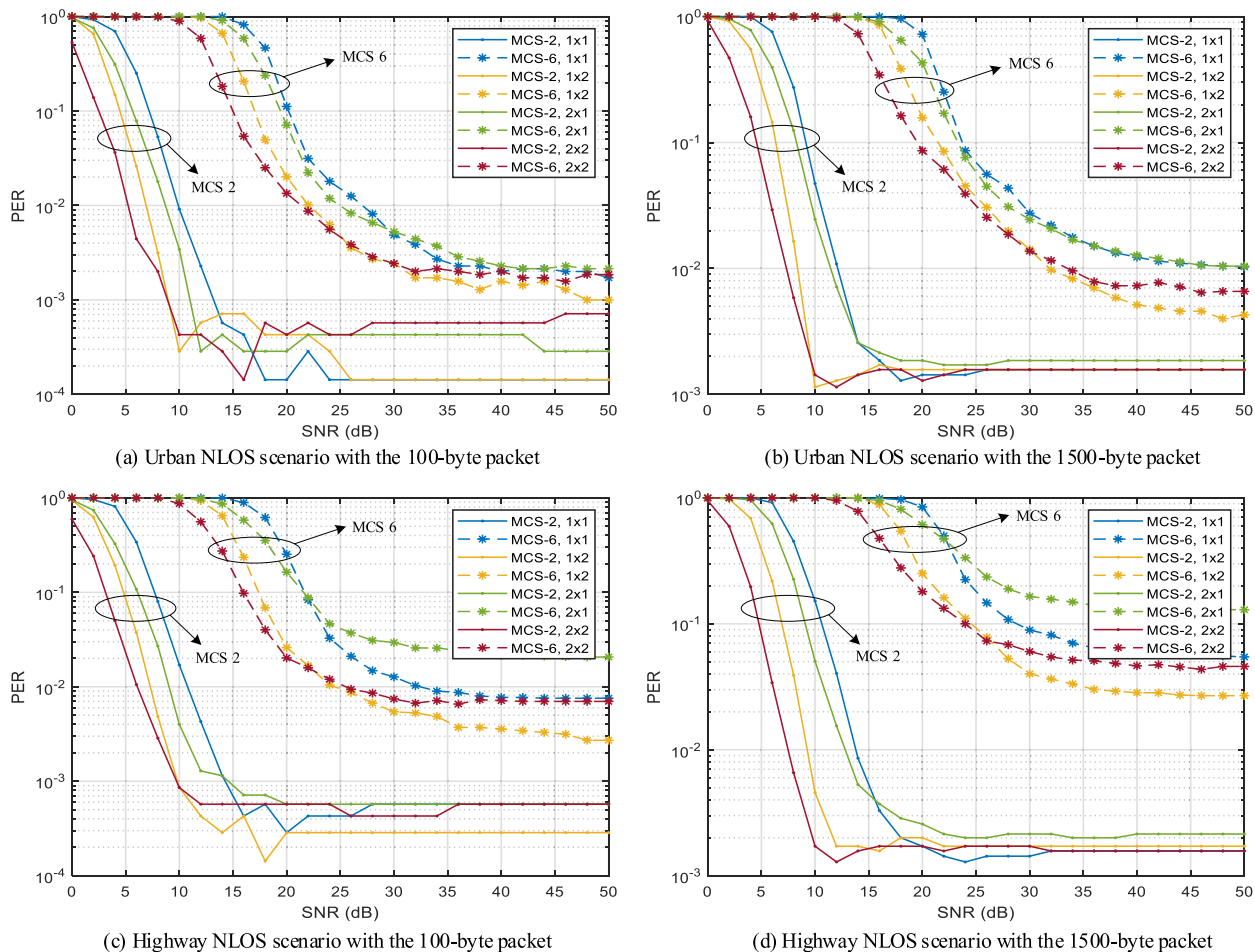


FIGURE 5. PER in urban NLOS and highway NLOS scenarios with the 100-byte and 1500-byte packets.

With both packet sizes, both MCSs, and both scenarios, the PER initially experiences a monotonic decrease with an increase of the SNR and finally achieves saturation at a high-SNR range in the SISO system.

b: MISO

When there are multiple antennas arranged in a transmitter, a transmit diversity can be realized by the MISO (2 × 1) system and thus the PER can be lowered in comparison with the SISO system.

The PER maintains the monotonic decline for the ascending SNR within a low-SNR range that is followed by the saturation obtained at higher SNR for all situations investigated in the MISO system.

c: SIMO

If a receiver is configured with multiple antennas, the PER in the SIMO (1 × 2) system whose receive diversity has been leveraged becomes further lower than that in the MISO system.

For both packet sizes with both MCSs in both scenarios, the PER starts from the monotonic drop with the growth of

the SNR and falls into saturation eventually in the SIMO system.

Although there are equal multiple antennas at the transmitter in the MISO system and at the receiver in the SIMO system, the SIMO system is still better than the MISO system whose channel state information (CSI) is unknown at the transmitter which leads to a higher PER [30].

d: MIMO

Once multiple antennas are deployed at the transmitter and receiver, both the transmit diversity and receive diversity are developed and thus the MIMO (2 × 2) system performs best relying on its lowest PER.

The PER for the MIMO system keeps descending monotonically with the increasing SNR until the emergence of saturation under all the observed conditions.

When the receiver and transmitter are far away from each other, the multi-antenna systems embody their benefits at low SNR to exploit the multipath components. Accordingly, in a low-SNR range which is defined below a specific SNR threshold shown in Table 5, the MIMO system is the best, the SIMO system is the better, the MISO system is the worse,

TABLE 5. SNR thresholds (dB) for PER.

V2V Scenario	100 bytes		1500 bytes	
	MCS 2	MCS 6	MCS 2	MCS 6
Urban NLOS	9.2	25.2	9.6	30.3
Highway NLOS	10	21.8	15	22.3

and the SISO system is the worst, regarding the reliability performance.

However, while the receiver gets closer to the transmitter, the interference among multiple antennas becomes predominant at high SNR. Consequently, the saturated PER in the MIMO, SIMO, or MISO system may be higher than that in the SISO system which breaks the fixed relationship of all the systems within the low-SNR range.

2) IMPACT OF PACKET SIZE

a: 100-BYTE PACKET

Beginning at a monotonic reduction with a growth of the SNR and ending at saturation, the 100-byte packet basically brings a lower PER and thus fulfills a higher reliability requirement in contrast with the 1500-byte packet. In addition, the smaller packet is less susceptible to the higher MCS and higher Doppler effect. Consequently, the smaller packet is preferred in the high-reliability communications, e.g., URLLC applications.

Furthermore, the SNR threshold with the 100-byte packet is always lower than that with the 1500-byte packet, which discloses that the multi-antenna systems are superior within a smaller low-SNR range for the smaller packet.

b: 1500-BYTE PACKET

By means of the initial monotonic decline and final saturation with the rising SNR, the PER is increased and hence the reliability is lower than that with the 100-byte packet.

Moreover, the more severe deterioration emerges for the higher MCS and higher Doppler effect.

3) IMPACT OF MCS

a: MCS 2

During an initial monotonic fall and a following saturation with an increase of the SNR, the lower PER is generally caused by MCS 2 and thus the reliability is enhanced accordingly. Moreover, the lower MCS is more resilient to the larger packet and higher Doppler effect. Therefore, the lower MCS is recommended in the ultra-reliable applications.

Besides, the SNR threshold for MCS 2 is greatly reduced and the low-SNR range where the multi-antenna systems are beneficial is shortened significantly.

b: MCS 6

According to the beginning monotonic decrease which is followed by eventual saturation with the growing SNR, the PER is elevated and hence the reliability is lowered for MCS 6.

TABLE 6. Impact of parameters on PER.

Parameter	PER
Antenna Configuration	MIMO<SIMO<MISO<SISO (Below SNR threshold)
Packet Size	100 bytes<1500 bytes (Mostly)
MCS	MCS 2<MCS 6 (Mostly)
V2V Scenario	Urban NLOS<Highway NLOS (Mostly)

Furthermore, the degradation gets worse for the larger packet and higher Doppler effect.

4) IMPACT OF V2V SCENARIO

a: URBAN NLOS SCENARIO

Under the urban scenario with a lower Doppler effect, the PER undergoes a monotonic decline with a rise of the SNR at lower SNR and enters saturation at higher SNR.

Moreover, the urban NLOS scenario usually possesses the slightly lower PER and is more tolerant to the larger packet and higher MCS compared to the highway NLOS scenario.

Additionally, the SNR threshold below which the PER of all the systems can be separated is lower for MCS 2 and higher for MCS 6 than that in the highway NLOS scenario. Therefore, the multi-antenna systems are favorable within a smaller low-SNR range for MCS 2 and within a larger low-SNR range for MCS 6.

b: HIGHWAY NLOS SCENARIO

With faster vehicles which result in a higher Doppler effect, the PER in the highway scenario remains the monotonic reduction with the ascending SNR before saturation.

Nevertheless, its PER is often a little higher and the larger packet as well as higher MCS are less endurable compared with the urban NLOS scenario.

The impact of all the analyzed parameters on the PER are summarized in Table 6.

B. PRR

Under the observed configurations and scenarios, the simulation results of the PRR are demonstrated in Fig.6 where there are merely MCS 2 and MCS 6 shown for convenience.

1) IMPACT OF ANTENNA CONFIGURATION

a: SISO

Without exploitation of any diversity, the lowest PRR and smallest transmission coverage are uncovered in the SISO (1 × 1) system which is the least beneficial in all the antenna configurations.

Moreover, the PRR always undergoes a monotonic rise with a decline of distance and becomes stable at a short-distance range in the SISO system for all the investigated conditions.

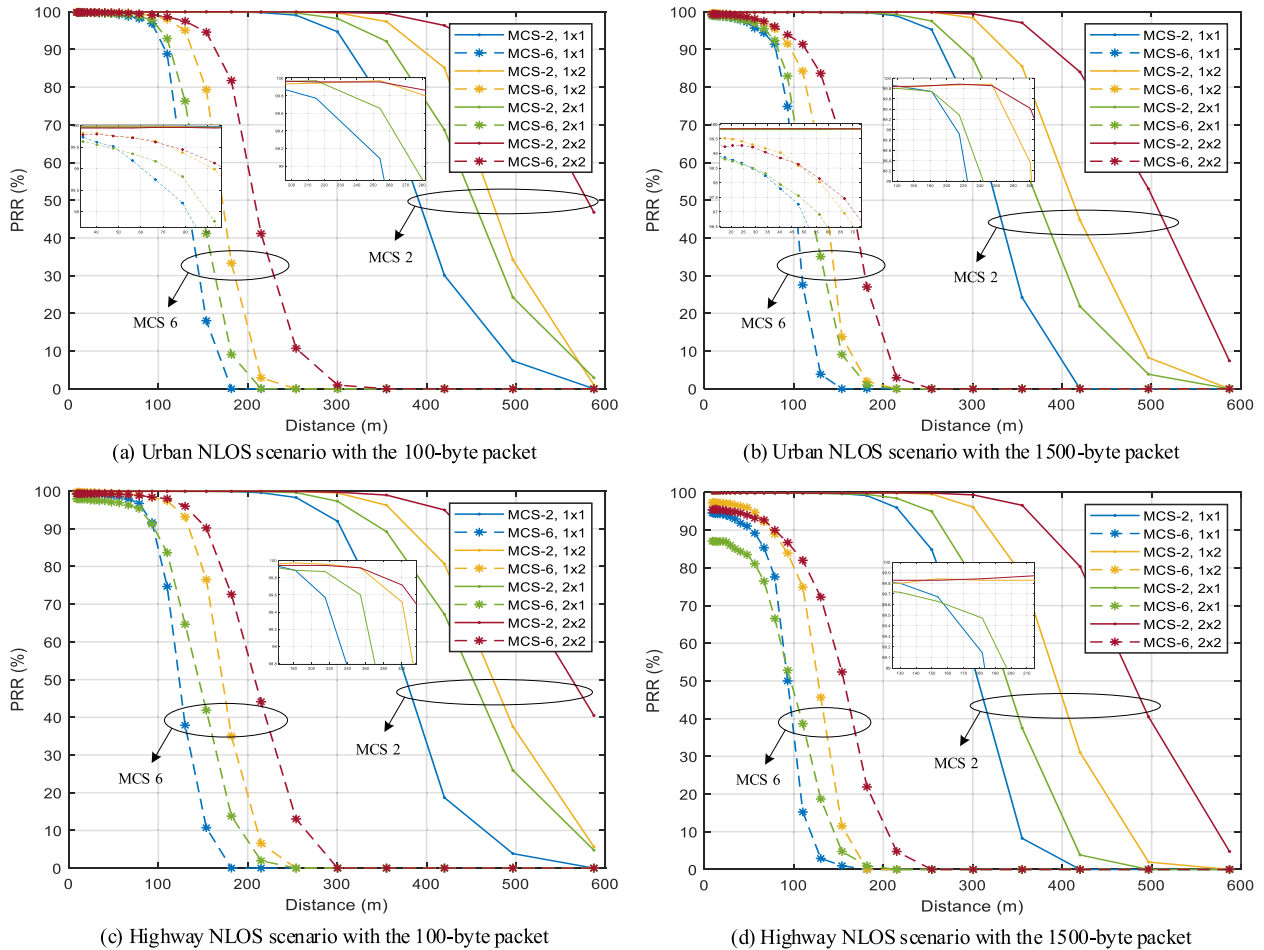


FIGURE 6. PRR in urban NLOS and highway NLOS scenarios with the 100-byte and 1500-byte packets.

b: MISO

Relying on the higher PRR and larger coverage, the MISO (2 × 1) system is superior to the SISO system.

Besides, the monotonic increase of the PRR with the descending distance is terminated with stability for short distance in the MISO system.

c: SIMO

Since the PRR and coverage are further improved, the SIMO (1 × 2) system is preferable to the MISO system.

Additionally, the PRR for the SIMO system is monotonically ascending with the reduction of the distance until its encounter with stability at short distance.

d: MIMO

Based on the most sufficient utilization of diversity, the MIMO (2 × 2) system is the most favorable with the highest PRR and largest coverage.

Furthermore, the monotonic growth of the PRR with the decreasing distance is continued with stability ultimately in the MIMO system.

TABLE 7. Basic coverages (m) with 90% PRR requirement.

V2V Scenario	100 bytes		1500 bytes	
	MCS 2	MCS 6	MCS 2	MCS 6
Urban NLOS	313	108	265	80
Highway NLOS	305	95	236	N/A

To completely and consistently evaluate the coverage with the specific packet size, MCS, and Doppler effect in various antenna configurations, the basic coverage, which can be guaranteed by all the antenna configurations, is defined as the minimum coverage in the MIMO, SIMO, MISO, and SISO systems. Specifically, the basic coverages which can meet the requirement on 90% PRR for the given packet and MCS configurations under both NLOS scenarios are listed in Table 7.

Corresponding to the PER of MCS 6 for the 2 × 1 system which is always higher than 10⁻¹ with the 1500-byte packet under the highway NLOS scenario, the resulting PRR is always lower than 90% and the basic coverage for the 90% PRR requirement does not exist due to the lack of generality.

TABLE 8. Distance thresholds (m) for PRR.

V2V Scenario	100 bytes		1500 bytes	
	MCS 2	MCS 6	MCS 2	MCS 6
Urban NLOS	259	70	255	46
Highway NLOS	254	94	168	90

Different from the short-distance range where the multi-antenna interference is dominant and may lead to a lower PRR and a smaller coverage in the MIMO, SIMO, or MISO system than that in the SISO system, the multi-antenna systems become favorable in utilizing the multipath at far distance. Consequently, the PRR and coverage performances in the MIMO, SIMO, MISO, and SISO systems are the best, better, worse, and worst respectively, within a far-distance range above a specific distance threshold listed in Table 8.

2) IMPACT OF PACKET SIZE

a: 100-BYTE PACKET

The PRR with the 100-byte packet initiates a monotonic rise with a reduction of distance and proceeds with stability.

Usually, higher PRR and larger coverage can be reached which lead to an expansion of the basic coverage. Hence, its basic coverage is always larger than that with the 1500-byte packet under all the investigated conditions. Besides, the smaller packet is more resistant to the higher MCS and higher Doppler effect. Accordingly, the basic coverage is still valid for 95 m although the MCS 6 and highway NLOS scenario are adopted.

Furthermore, the higher distance threshold for the 100-byte packet narrows the far-distance range where the multi-antenna systems are beneficial.

b: 1500-BYTE PACKET

During the monotonic growth and succeeding stability with the descending distance, the PRR is reduced and hence the coverage is diminished for the 1500-byte packet.

More affected by the higher MCS and higher Doppler effect, the basic coverage for MCS 6 under the highway NLOS scenario is disabled.

3) IMPACT OF MCS

a: MCS 2

The PRR of MCS 2 begins with a monotonic increase and terminates with stability along with a decrease of distance.

The PRR is often elevated, hence, the coverage is enlarged which gives rise to a larger basic coverage. Accordingly, its basic coverage is significantly greater than that for MCS 6. Less vulnerable to the larger packet and higher Doppler effect, the basic coverage of 236 m can still be realized even if the 1500-byte packet and highway NLOS scenario are encountered.

TABLE 9. Impact of parameters on PRR.

Parameter	PRR
Antenna Configuration	MIMO>SIMO>MISO>SISO (Above distance threshold)
Packet Size	100 bytes>1500 bytes (Mostly)
MCS	MCS 2>MCS 6 (Mostly)
V2V Scenario	Urban NLOS>Highway NLOS (Mostly)

Moreover, the distance threshold is extremely higher for MCS 2 which remarkably limits the far-distance range where the multi-antenna systems are favorable.

b: MCS 6

Based on the initial monotonic growth and final stability with the reducing distance, the PRR gets lower and hence the coverage becomes smaller compared to that with MCS 2.

More influenced by the larger packet and higher Doppler effect, the basic coverage is invalid in the highway NLOS scenario with the 1500-byte packet.

4) IMPACT OF V2V SCENARIO

a: URBAN NLOS SCENARIO

The PRR in the urban NLOS scenario initially experiences a monotonic increase and then remains stable with a decline of distance.

Generally, the PRR is slightly higher, and the coverage is somewhat extended accordingly. As a result, the basic coverage is also extended with a simultaneous expansion of the coverages in all antenna configurations. Consequently, its basic coverage is always larger than that in the highway NLOS scenario for all the observed situations. Moreover, the urban NLOS scenario is less sensitive to the larger packet and higher MCS. Thus, the basic coverage can still reach as far as 80 m even for MCS 6 with the 1500-byte packet.

The distance threshold of the PRR is higher for MCS 2 and lower for MCS 6 in contrast with the highway NLOS scenario. Accordingly, the multi-antenna systems are conducive within a smaller far-distance range for MCS 2 and within a larger far-distance range for MCS 6.

b: HIGHWAY NLOS SCENARIO

Experiencing monotonic growth and subsequent stability with the decrease in distance, the PRR is lowered and thus the coverage is shortened in the highway NLOS scenario.

Less tolerable to the larger packet and higher MCS, the basic coverage for MCS 6 with the 1500-byte packet cannot be realized.

The impact of all the analyzed parameters on the PRR are summarized in Table 9.

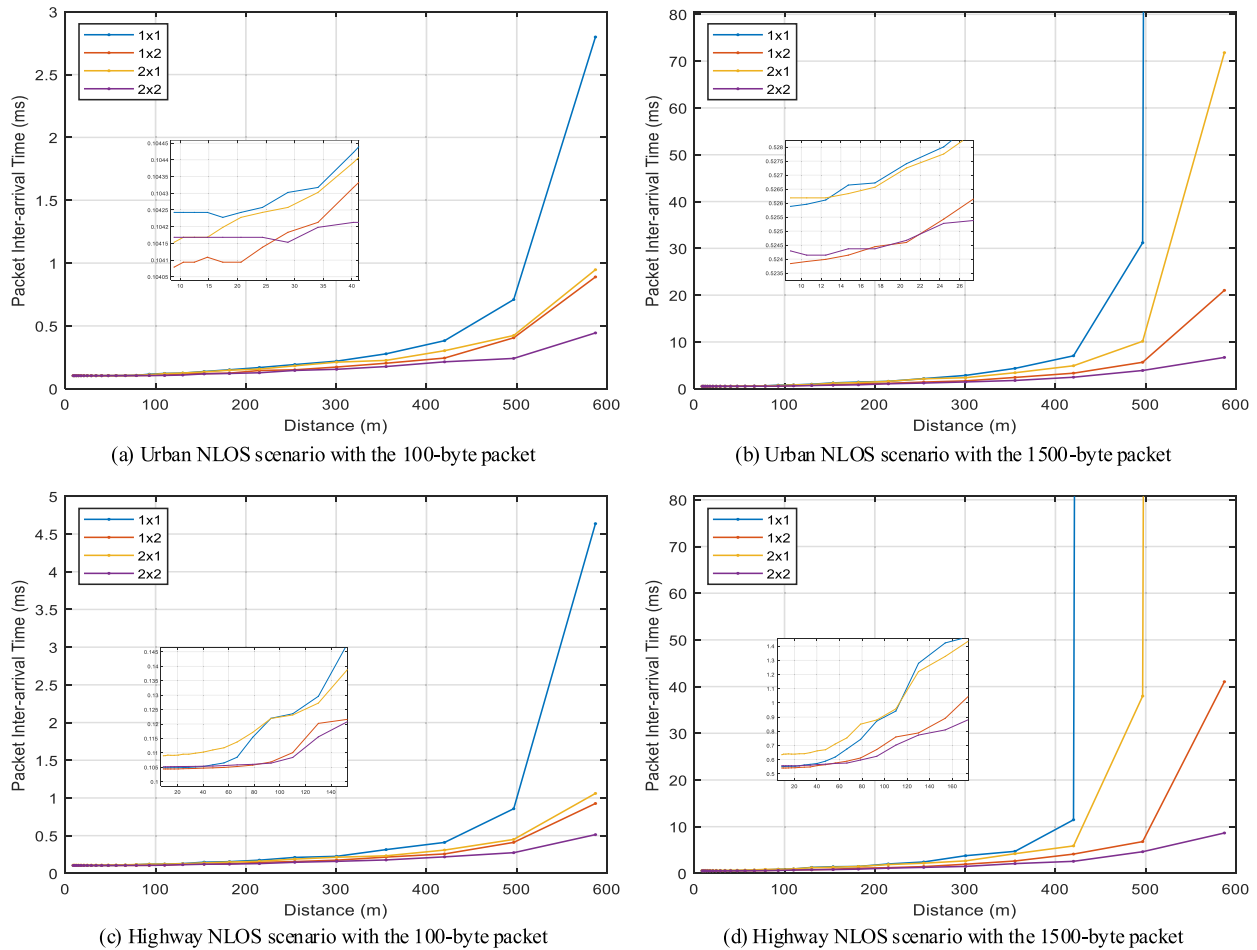


FIGURE 7. Output packet IAT in urban NLOS and highway NLOS scenarios with the 100-byte and 1500-byte packets.

C. OUTPUT PACKET IAT

Due to the variation on distance between the receiver and transmitter which results in changing SNRs with different channel fading conditions, the output packet IAT, which is defined as the minimum packet IAT for all MCSs, can be obtained in the link adaptation at each observed distance which can better accommodate the channel characteristics [19].

With the given antenna and packet configurations under both NLOS scenarios, the simulation results of the output packet IAT are exhibited in Fig. 7.

1) IMPACT OF ANTENNA CONFIGURATION

a: SISO

The output packet IAT is monotonically decreasing with a reduction of distance in the SISO (1×1) system for all the considered situations and remains largest among all the antenna configurations above a specific distance threshold.

Most vulnerable to the larger packet, the output packet IAT with the 1500-byte packet suffers from an abrupt growth with the increasing distance not only under the highway NLOS scenario but also under the urban NLOS scenario, and

both the resulting output packet IATs approach infinity at far distance.

b: MISO

Based on the monotonic decline with the descending distance, the output packet IAT is decreased in the MISO (2×1) system than that in the SISO system above the distance threshold.

More sensitive to the larger packet and higher Doppler effect, the output packet IAT with the 1500-byte packet under the highway NLOS scenario is close to infinity after the steep increase with the ascending distance at far distance.

c: SIMO

The output packet IAT follows the monotonic decrease with the reducing distance in the SIMO (1×2) system and is further reduced in comparison to the MISO system above the distance threshold.

d: MIMO

According to the monotonic reduction with the diminishing distance, the output packet IAT is smallest in the MIMO ($2 \times$

TABLE 10. Distance thresholds (m) for output packet IAT.

V2V Scenario	100 bytes	1500 bytes
Urban NLOS	27	22
Highway NLOS	93	114

2) system which outperforms the SIMO, MISO, and SISO systems above the distance threshold.

Contrary to the multi-antenna configurations that may lead to a larger output packet IAT in comparison to the single-antenna configuration because of the interference generated at short distance, the multi-antenna systems become beneficial in applying the multipath components over long distance. Accordingly, the MIMO, SIMO, MISO, and SISO systems perform best, better, worse, and worst respectively, on the output packet IAT in the long-distance range above the distance threshold demonstrated in Table 10.

2) IMPACT OF PACKET SIZE

a: 100-BYTE PACKET

The output packet IAT with the 100-byte packet follows a monotonic decrease with a decline in distance gradually and is always smaller than that with the 1500-byte packet which is preferable for low-latency communications. Less susceptible to the higher Doppler effect, the degeneration on the output packet IAT in the highway NLOS scenario is effectively suppressed and an infinite output packet IAT at far distance can be avoided for both scenarios.

The distance threshold with the 100-byte packet which is lower in the highway NLOS scenario and higher in the urban NLOS scenario compared to the 1500-byte packet respectively expands and shortens the far-distance range where the multi-antenna systems are favorable.

b: 1500-BYTE PACKET

After the steep and monotonic growth of the output packet IAT with increasing distance, the resulting output packet IAT with the 1500-byte packet is extremely higher than that with the 100-byte packet and the infinite output packet IAT appears in both the urban NLOS and highway NLOS scenarios over long distance. Furthermore, the gap between both scenarios is enlarged with the larger packet.

3) IMPACT OF V2V SCENARIO

a: URBAN NLOS SCENARIO

The output packet IAT undergoes a monotonic drop with a decrease in distance and is usually smaller compared to the highway NLOS scenario. More tolerant to the larger packet, the advantage of the urban NLOS scenario over the highway NLOS scenario becomes more prominent with the 1500-byte packet.

Additionally, the much smaller distance threshold greatly extends the far-distance range where the multi-antenna systems are conducive.

TABLE 11. Impact of parameters on output packet IAT.

Parameter	Output Packet IAT
Antenna Configuration	MIMO<SIMO<MISO<SISO (Above distance threshold)
Packet Size	100 bytes<1500 bytes (Always)
V2V Scenario	Urban NLOS<Highway NLOS (Mostly)

b: HIGHWAY NLOS SCENARIO

During the monotonic decline with the reducing distance, the increase of the output packet IAT compared with the urban NLOS scenario is more remarkable with the 1500-byte packet. Accordingly, the infinite output packet IAT at far distance occurs in both the 1×1 and 2×1 systems after more dramatic rise with the increase of the distance for the highway NLOS scenario but exclusively in the 1×1 system for the urban NLOS scenario.

The impact of all the analyzed parameters on the output packet IAT are summarized in Table 11.

D. OUTPUT EFFECTIVE DATA RATE

Since the SNR is varying with changing distances and channel fading conditions, the output effective data rate, defined as the maximum effective data rate for all MCSs, can be caught by the link adaptation at each specified distance [19], [21].

For the specific antenna and packet configurations in both NLOS scenarios, the simulation results of the output effective data rate are illustrated in Fig. 8.

1) IMPACT OF ANTENNA CONFIGURATION

a: SISO

The output effective data rate is monotonically increasing with a decline in distance under all the observed cases in the SISO (1×1) system and stays lowest in all the antenna configurations above a specific distance threshold.

b: MISO

According to the monotonic rise with the diminishing distance, the output effective data rate is improved in the MISO (2×1) system compared with the SISO system above the distance threshold.

c: SIMO

During the monotonic increase with the descending distance, the output effective data rate can be further enhanced in the SIMO (1×2) system compared with the MISO system above the distance threshold.

d: MIMO

The output effective data rate is monotonically growing with the decreasing distance in the MIMO (2×2) system and

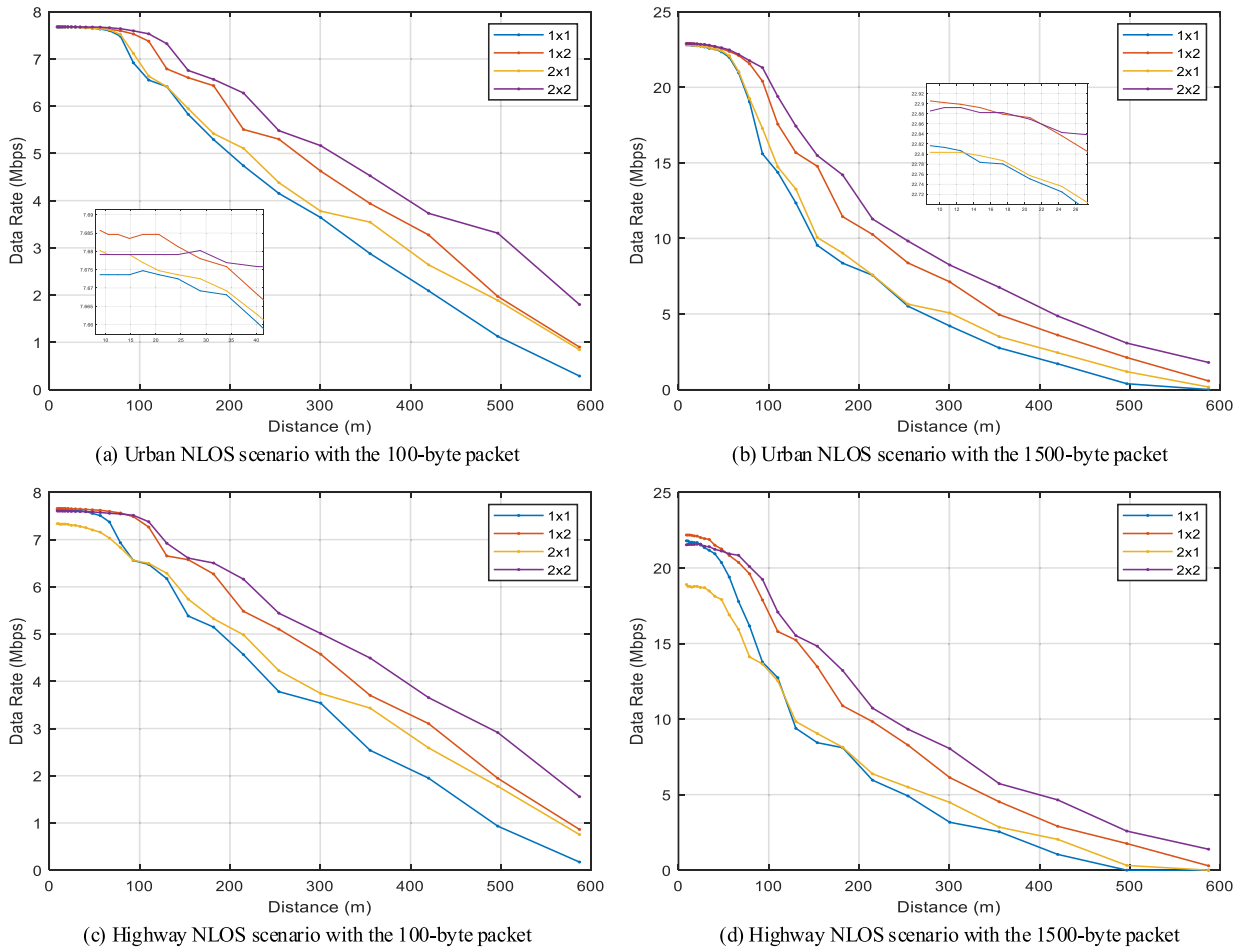


FIGURE 8. Output effective data rate in urban NLOS and highway NLOS scenarios with the 100-byte and 1500-byte packets.

TABLE 12. Distance thresholds (m) for output effective data rate.

V2V Scenario	100 bytes	1500 bytes
Urban NLOS	27	22
Highway NLOS	93	116

surpasses that from all the other systems above the distance threshold.

Instead of the interference which occurs within short distance and sometimes generates lower output effective data rate in the multi-antenna configurations in comparison to the single-antenna configuration, the multipath components can be exerted in the multi-antenna systems over long distance. Consequently, the best, better, worse, and worst performances on the output effective data rate are exhibited in the MIMO, SIMO, MISO, and SISO systems respectively at the far-distance range above the distance threshold illustrated in Table 12.

2) IMPACT OF PACKET SIZE

a: 100-BYTE PACKET

The output effective data rate with the 100-byte packet, which is often lower than that with the 1500-byte packet,

experiences a monotonic rise with a decrease in distance gently. More resilient to the higher Doppler effect, the gap can be constrained significantly between the highway NLOS scenario and urban NLOS scenario.

The distance threshold with the 100-byte packet that is lower for the highway NLOS scenario and higher for the urban NLOS scenario compared to the 1500-byte packet respectively represents the larger and smaller far-distance range where the multi-antenna systems are beneficial.

b: 1500-BYTE PACKET

Due to a sharp increase, which is monotonic, with the decline in distance, the higher output effective data rate still can be obtained with the 1500-byte packet for the majority in distance even though the minimum output effective data rate over the farthest distance is close to that with the 100-byte packet. Thus, the larger packet maintains its superiority in the high-throughput applications.

Besides, the degradation on the output effective data rate with the higher Doppler effect becomes worse with the larger packet and the extraordinary distinction exists at short distance within 100 m between both scenarios.

TABLE 13. Impact of parameters on output effective data rate.

Parameter	Output Effective Data Rate
Antenna Configuration	MIMO>SIMO>MISO>SISO (Above distance threshold)
Packet Size	1500 bytes>100 bytes (Mostly)
V2V Scenario	Urban NLOS>Highway NLOS (Mostly)

3) IMPACT OF V2V SCENARIO

a: URBAN NLOS SCENARIO

The output effective data rate always follows a monotonic growth with a reduction in distance for the urban NLOS scenario and is generally higher than that for the highway NLOS scenario. With more superiority than the highway NLOS scenario for the larger packet, the urban NLOS scenario is more resistant to the challenging large packet.

In addition, the distance threshold is much smaller and hence the multi-antenna systems are beneficial within a rather longer far-distance range.

b: HIGHWAY NLOS SCENARIO

Based on the monotonic increase with the descending distance, the deterioration in the output effective data rate under the highway NLOS scenario emerges and becomes more serious with the larger packet. Specifically, compared to the urban NLOS scenario whose initial output effective data rates with the 1500-byte packet are always higher than 22 Mbps, the initial output effective data rates with the 1500-byte packet under the highway NLOS scenario drop slightly in the 1×1 and 2×2 systems which are merely below 22 Mbps and seriously in the 2×1 system which is even below 19 Mbps.

The impact of all the analyzed parameters on the output effective data rate are summarized in Table 13.

V. CONCLUSION

In this paper, the complete PHY performance of IEEE 802.11p is sufficiently investigated and evaluated in terms of the PER, PRR, output packet IAT, and output effective data rate. Various antenna, packet, and MCS configurations are studied under both the urban NLOS and highway NLOS scenarios to explore the impact of the antenna configuration, packet size, MCS, and Doppler effect on the PHY performance. The detailed conclusions are summarized as follows, which can be compared with that on IEEE 802.11bd in our previous work [19].

- The MIMO system performs best with the lowest PER, largest PRR as well as transmission coverage, smallest output packet IAT, and highest output effective data rate, at the distance above the distance threshold which corresponds to the SNR below the SNR threshold [32]. On the contrary, the SISO system is the least beneficial with the worst performance and most vulnerable to the

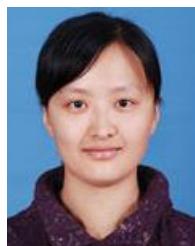
larger packet, higher MCS, and higher Doppler effect. The performances of the SIMO and MISO systems are in between that of the MIMO and SISO systems, and the SIMO system is better than the MISO system although there are equal multiple antennas at the transmitter in the MISO system and at the receiver in the SIMO system.

- The smaller packet, which is less sensitive to the higher MCS and higher Doppler effect, is more favorable for the high-reliability and low-latency communications based on its lower PER, larger PRR and transmission coverage, and smaller output packet IAT. Meanwhile, the larger packet that can achieve a higher output effective data rate is more beneficial in the high-throughput communications.
- The lower MCS, that is less susceptible to the larger packet and higher Doppler effect, is more conducive in the high-reliability communications due to its lower PER, higher PRR, and larger transmission coverage. On the other hand, the higher MCS can realize the smaller output packet IAT for the low-latency communications and the higher output effective data rate for the high-throughput communications.
- Depending on the slight superiority in reducing the PER, increasing the PRR and transmission coverage, decreasing the output packet IAT, and enhancing the output effective data rate compared to the highway NLOS scenario with higher Doppler effect, the urban NLOS scenario with lower Doppler effect is more resistant to the larger packet and higher MCS.

REFERENCES

- [1] F. Arena, G. Pau, and A. Severino, "A review on IEEE 802.11p for intelligent transportation systems," *J. Sensor Actuator Netw.*, vol. 9, no. 2, p. 22, Apr. 2020.
- [2] X. Huang, D. Zhao, and H. Peng, "Empirical study of DSRC performance based on safety pilot model deployment data," *IEEE Trans. Intell. Transp. Syst.*, vol. 18, no. 10, pp. 2619–2628, Oct. 2017.
- [3] W. Anwar, S. Dev, A. Kumar, N. Franchi, and G. Fettweis, "PHY abstraction techniques for V2X enabling technologies: Modeling and analysis," *IEEE Trans. Veh. Technol.*, vol. 70, no. 2, pp. 1501–1517, Feb. 2021.
- [4] G. Naik, B. Choudhury, and J.-M. Park, "IEEE 802.11bd & 5G NR V2X: Evolution of radio access technologies for V2X communications," *IEEE Access*, vol. 7, pp. 70169–70184, 2019.
- [5] J. Choi, V. Marojevic, C. B. Dietrich, J. H. Reed, and S. Ahn, "Survey of spectrum regulation for intelligent transportation systems," *IEEE Access*, vol. 8, pp. 140145–140160, 2020.
- [6] *IEEE Standard for Information Technology-Telecommunications and Information Exchange Between Systems Local and Metropolitan Area Networks-Specific Requirements—Part 11: Wireless LAN Medium Access Control (MAC) and Physical Layer (PHY) Specifications*, IEEE Standard 802.11-2020 (Revision of IEEE Std 802, Nov. 2020).
- [7] *TSG SA, Release Description; Release 14*, document TR 21.914, V14.0.0, 3GPP, Jun. 2018.
- [8] B. Sadeghi, *802.11bd Specification Framework Document*, Standard 802.11-15/0132r07, Sep. 2019.
- [9] *IEEE Standard for Information Technology-Telecommunications and Information Exchange Between Systems Local and Metropolitan Area Networks-Specific Requirements—Part 11: Wireless LAN Medium Access Control (MAC) and Physical Layer (PHY) Specifications Amendment 5: Enhancements for Next Generation V2X*, IEEE Standard 802.11bd, 2022.
- [10] *TSG SA, Release Description; Release 16*, document TR 21.916, V16.2.0, Jun. 2022.

- [11] N. Patriciello, S. Lagen, B. Bojovic, and L. Giupponi, "An E2E simulator for 5G NR networks," *Simul. Model. Pract. Theory*, vol. 96, Nov. 2019, Art. no. 101933.
- [12] A. Bazzi, B. M. Masini, A. Zanella, and I. Thibault, "On the performance of IEEE 802.11p and LTE-V2V for the cooperative awareness of connected vehicles," *IEEE Trans. Veh. Technol.*, vol. 66, no. 11, pp. 10419–10432, Nov. 2017.
- [13] K. Kiela, V. Barzdenas, M. Jurgo, V. Macaitis, J. Rafanavicius, A. Vasjanov, L. Kladovcikov, and R. Navickas, "Review of V2X-IoT standards and frameworks for ITS applications," *Appl. Sci.*, vol. 10, no. 12, p. 4314, Jun. 2020.
- [14] A. Bazzi, G. Cecchini, M. Menarini, B. M. Masini, and A. Zanella, "Survey and perspectives of vehicular Wi-Fi versus sidelink cellular-V2X in the 5G era," *Future Internet*, vol. 11, no. 6, p. 122, May 2019.
- [15] Z. H. Mir and F. Filali, "LTE and IEEE 802.11p for vehicular networking: A performance evaluation," *EURASIP J. Wireless Commun. Netw.*, vol. 2014, no. 1, p. 89, May 2014.
- [16] A. Triwinarko, I. Dayoub, and S. Cherkaoui, "PHY layer enhancements for next generation V2X communication," *Veh. Commun.*, vol. 32, Dec. 2021, Art. no. 100385.
- [17] X. Ma and K. S. Trivedi, "SINR-based analysis of IEEE 802.11p/bd broadcast VANETs for safety services," *IEEE Trans. Netw. Service Manage.*, vol. 18, no. 3, pp. 2672–2686, Sep. 2021.
- [18] K. Ansari, "Joint use of DSRC and C-V2X for V2X communications in the 5.9 GHz ITS band," *IET Intell. Transp. Syst.*, vol. 15, no. 2, pp. 213–224, Feb. 2021.
- [19] S. Guo, D. N. Aloï, J. Li, and H. Zhao, "MIMO-based physical layer evaluation on IEEE 802.11bd," *IEEE Access*, vol. 11, pp. 115511–115528, 2023.
- [20] R. Liu and D. N. Aloï, "A rigorous analysis of vehicle-to-vehicle range performance in a rural channel propagation scenario as a function of antenna type and location via simulation and field trials," *China Commun.*, vol. 20, no. 11, pp. 131–141, Nov. 2023.
- [21] W. Anwar, N. Franchi, and G. Fettweis, "Physical layer evaluation of V2X communications technologies: 5G NR-V2X, LTE-V2X, IEEE 802.11bd, and IEEE 802.11p," in *Proc. IEEE 90th Veh. Technol. Conf. (VTC-Fall)*, Sep. 2019, pp. 1–7.
- [22] T. Petrov, L. Sevcik, P. Pocta, and M. Dado, "A performance benchmark for dedicated short-range communications and LTE-based cellular-V2X in the context of vehicle-to-infrastructure communication and urban scenarios," *Sensors*, vol. 21, no. 15, p. 5095, Jul. 2021.
- [23] J. Zhao, X. Gai, and X. Luo, "Performance comparison of vehicle networking based on DSRC and LTE technology," in *Proc. 6th Int. Conf. Intell. Transp. Eng. (ICITE)*, Z. Zhang, Ed., Singapore: Springer, Jan. 2022, pp. 730–746.
- [24] R. Jacob, W. Anwar, N. Schwarzenberg, N. Franchi, and G. Fettweis, "System-level performance comparison of IEEE 802.11p and 802.11bd draft in highway scenarios," in *Proc. 27th Int. Conf. Telecommun. (ICT)*, Oct. 2020, pp. 1–6.
- [25] D. Shukla, V. Kumar, and A. Prakash, "Performance evaluation of IEEE 802.11p physical layer for efficient vehicular communication," in *Advances in VLSI, Communication, and Signal Processing*, D. Dutta, H. Kar, C. Kumar, and V. Bhadauria, Eds., Singapore: Springer, 2020, pp. 51–60.
- [26] A. Grami, *Introduction to Digital Communications*. Oxford, U.K.: Academic Press, 2016, pp. 493–511.
- [27] V. K. Garg, *Wireless Communications and Networking*. San Francisco, CA, USA: Morgan Kaufmann, 2007, pp. 47–84.
- [28] A. Bensky, *Short-Range Wireless Communication*, 3rd ed., Oxford, U.K.: Newnes, 2019, pp. 11–41.
- [29] B. Sklar and F. J. Harris, *Digital Communications: Fundamentals and Applications*, 3rd ed., Hoboken, NJ, USA: Pearson, 2021, pp. 971–1088.
- [30] T.-D. Chiueh, P.-Y. Tsai, and I.-W. Lai, *Baseband Receiver Design for Wireless MIMO-OFDM Communications*, 2nd ed., Singapore: Wiley, 2012, pp. 39–53.
- [31] A. Zaidi, F. Athley, J. Medbo, U. Gustavsson, G. Durisi, and X. Chen, *5G Physical Layer: Principles, Models and Technology Components*. Oxford, U.K.: Academic Press, 2018, pp. 119–125.
- [32] L. Hanzo, Y. Akhtman, L. Wang, and M. Jiang, *MIMO-OFDM for LTE, Wi-Fi and WiMAX: Coherent Versus Non-Coherent and Cooperative Turbo-Transceivers*. Chichester, U.K.: Wiley, 2011, pp. 1–36.
- [33] T. Hwang, C. Yang, G. Wu, S. Li, and G. Ye Li, "OFDM and its wireless applications: A survey," *IEEE Trans. Veh. Technol.*, vol. 58, no. 4, pp. 1673–1694, May 2009.
- [34] H. Asplund, D. Astely, P. von Butovitsch, T. Chapman, M. Frenne, F. Ghasemzadeh, M. Hagström, B. Hogan, G. Jöngren, J. Karlsson, F. Kronstedt, and E. Larsson, *Advanced Antenna Systems for 5G Network Deployments: Bridging the Gap between Theory and Practice*. Oxford, U.K.: Academic Press, 2020, pp. 133–159.
- [35] A. Paulraj, R. Nabar, and D. Gore, *Introduction to Space-Time Wireless Communications*. Cambridge, U.K.: Cambridge Univ. Press, 2003, pp. 178–198.
- [36] T. J. Roupheal, *RF and Digital Signal Processing for Software-Defined Radio: A Multi-Standard Multi-Mode Approach*. Oxford, U.K.: Newnes, 2009, pp. 65–71.
- [37] S. Chen and A. M. Wyglinski, "Digital communication fundamentals for cognitive radio," in *Cognitive Radio Communications and Networks: Principles and Practice*, A. M. Wyglinski, M. Nekovee, and T. Hou, Eds., Oxford, U.K.: Academic Press, 2010, pp. 57–72.
- [38] S. K. Wilson and O. A. Dobre, "Multicarrier transmission in a frequency-selective channel," in *Academic Press Library in Mobile and Wireless Communications: Transmission Techniques for Digital Communications*, S. K. Wilson, S. Wilson, and E. Biglieri, Eds., Oxford, U.K.: Academic Press, 2016, pp. 333–367.
- [39] C. F. Mecklenbrauker, A. F. Molisch, J. Karedal, F. Tufvesson, A. Paier, L. Bernado, T. Zemen, O. Klemp, and N. Czink, "Vehicular channel characterization and its implications for wireless system design and performance," *Proc. IEEE*, vol. 99, no. 7, pp. 1189–1212, Jul. 2011.
- [40] R. W. Heath Jr. and A. Lozano, *Foundations of MIMO Communication*. Cambridge, U.K.: Cambridge Univ. Press, 2019, pp. 77–110.
- [41] Z. Rafique and B.-C. Seet, "Energy-efficient MIMO-OFDM systems," in *Handbook of Green Information and Communication Systems*, M. S. Obaidat, A. Anpalagan, and I. Woungang, Eds., Oxford, U.K.: Academic Press, 2013, pp. 393–422.
- [42] K. Raoof, M. B. Zid, N. Prayongpun, and A. Bouallegue, "Advanced MIMO techniques: Polarization diversity and antenna selection," in *MIMO Systems, Theory and Applications*, H. K. Biazaki, Ed., Norderstedt, Germany: BoD-Books Demand, 2011, pp. 3–56.
- [43] S. Bartoletti, W. Zhuofei, V. Martinez, and A. Bazzi, "A physical layer model for the performance evaluation of V2X communication," *J. Latex Class Files*, vol. 14, no. 8, pp. 1–5, Aug. 2021.
- [44] M. Kahn, *V2V Radio Channel Models*, Standard 802.11-14/0259r0, Feb. 2014.
- [45] J. R. Hampton, *Introduction to MIMO Communications*. Cambridge, U.K.: Cambridge Univ. Press, 2014, pp. 1–69.
- [46] I. Sarris. (2020). *U-Blox/UBX-V2X [Source Code]*. [Online]. Available: <https://github.com/u-blox/ubx-v2x>
- [47] W. Anwar. (2020). *PHY Abstraction_V2X_technologies-IEEE-802.11p-IEEE802.11bd-LTE-V2X-NR-V2X- [Source Code]*. [Online]. Available: https://github.com/Waqar-Anwar/PHY_abstraction_V2X_technologies-IEEE-802.11p-IEEE802.11bd-LTE-V2X-NR-V2X-



SHUTING GUO received the B.S.E. degree in electronic information engineering from Henan Normal University, Xinxiang, Henan, China, in 2004, and the M.S.E. degree in signal and information processing from Xidian University, Xi'an, Shanxi, China, in 2008. She is currently pursuing the Ph.D. degree in electrical engineering with Oakland University, Rochester, MI, USA.

Since 2008, she has been a Lecturer with the Electrical and Information Engineering College, Zhengzhou University of Light Industry, Zhengzhou, Henan. Her research interests include the physical layer evaluation and analysis of V2X communications with IEEE 802.11p, IEEE 802.11bd, LTE-V2X, and 5G NR.



DANIEL N. ALOÏ (Senior Member, IEEE) received the B.S., M.S., and Ph.D. degrees in electrical engineering from Ohio University, Athens, OH, USA, in 1992, 1996, and 1999, respectively.

He was a Research Assistant with the Avionics Engineering Center, School of Engineering and Computer Science, Ohio University, from 1995 to 1999; a Summer Intern with Rockwell International, Cedar Rapids, Iowa, and a Senior Project Engineer with OnStar, Incorporated, a subsidiary of General Motors, from 2000 to 2002. He has been with the Electrical and Computer Engineering Department, Oakland University, Rochester, MI, USA, since 2002. He is the Founder and the Director of the Applied EMAG and Wireless Laboratory, Oakland University. He has received more than \$4M in research funding from a variety of federal and private entities including the Federal Aviation Administration, Defense Advanced Research Program Agency (DARPA), and the National Science Foundation (NSF). He has authored/co-authored more than 100 technical articles and is an inventor on five patents. His research interests include applied electromagnetics with an emphasis on antenna measurements, antenna modeling/analysis, and antenna design.

Dr. Aloï is a member of the Institute of Navigation.



JIA LI (Senior Member, IEEE) received the B.S. degree in electronics and information systems from Peking University, Beijing, China, in 1996, and the M.S.E. and Ph.D. degrees in electrical engineering from the University of Michigan, Ann Arbor, MI, USA, in 1997 and 2002, respectively.

She has been a Faculty Member with the School of Engineering and Computer Science, Oakland University, since 2002. Her past and current research are sponsored by NSF, NIH, General Motors, Fiat Chrysler, the National Research Council, and the Air Force Office of Scientific Research. She has authored/co-authored more than 90 refereed publications, including one book. Her research interests include statistical learning and signal processing with applications in radar, sensor fusion, communications, and biomedical imaging.

Dr. Li serves as a member of technical committees of several international conferences and workshops.



HONGMEI ZHAO received the B.S. degree in electrical engineering from the First Aviation University of Air Force, Xinyang, Henan, China, in 1999, and the Ph.D. degree in information and communication engineering from Nanjing University of Science and Technology, Nanjing, Jiangsu, China, in 2009.

From 1999 to 2003, she was an Assistant Engineer with Technical Section in Luohe People's Broadcasting Station, Luohe, Henan. She was an Associate Professor, from 2009 to 2018, and has been a Professor with Electrical and Information Engineering College, Zhengzhou University of Light Industry, Zhengzhou, Henan, since 2018. From 2017 to 2018, she was a Visiting Scholar with the Electrical and Computer Engineering Department, University of British Columbia, Vancouver, Canada. She is the author of two books, more than 40 articles, and 20 patents. Her research interests include the ultra-band indoor location systems, microstrip antenna, array signal processing, radio propagation, and wireless navigation and location technology application.

Dr. Zhao has four the second awards of the Science and Technology Progress Awards of Henan Province and more than six the first awards of the Outstanding Achievements in Science and Technology Award of the Education Department of Henan, China.

• • •